Prospects for Observing the Microquasar SS 433 with the LACT Array

Zhen Xie, 1, 2, 3 Zhipeng Zhang, 1, 2, 3 and Ruizhi Yang 1, 2, 3, *

¹School of Physical Sciences, University of Science and Technology of China, Hefei 230026, China ²School of Astronomy and Space Science, University of Science and Technology of China, Hefei, Anhui 230026, China ³Tianfu Cosmic Ray Research Center, Chengdu, China

We investigate the observational capabilities of the upcoming LACT Cherenkov telescope array for the microquasar SS 433 through detailed simulations. Our results indicate that a detection significance of about 5σ can be achieved with approximately 30 hours of observation. The array is capable of spatially resolving the eastern and western jets, and—based on the LHAASO spectral and morphological findings—can distinguish the central hadronic component after roughly 100 h of observation. We further examine its ability to distinguish between the H.E.S.S. and LHAASO spectral models. These findings demonstrate LACT's strong potential to probe the spatial and spectral structure of SS 433 at very high energies, providing valuable insights into particle acceleration in PeVatrons and the radiation mechanisms of microquasars.

INTRODUCTION

Astrophysical jets are among the most prominent manifestations of energy release in accreting compact objects. The first observational evidence of such jets dates back more than a century, with optical studies of the M87 galaxy revealing a collimated structure emerging from its nucleus [1]. The advent of radio astronomy in the 1930s enabled the discovery of many more jet-like sources [2], with a major breakthrough occurring in 1953 when Cygnus A, a bright radio galaxy, was resolved into two distinct lobes [3]. The subsequent identification of quasars in 1963 [4, 5] further established jets as a common feature of powerful astrophysical systems. Today, jets are observed across a wide range of environments, from active galactic nuclei [6] to microguasars [7], and are often associated with strong non-thermal emission [8]. The broadband radiation, extending from radio waves to gamma rays, provides direct evidence of particle acceleration to relativistic energies. Synchrotron radiation from relativistic electrons produces the radio to X-ray emission, while inverse Compton scattering [9] and hadronic interactions can contribute to high-energy and very-highenergy gamma-ray emission. The non-thermal nature of these emissions makes jets unique laboratories for studying extreme particle acceleration and radiation processes in astrophysical plasmas.

Evidence for particle acceleration in jets is abundant. Observational signatures such as non-thermal spectra [8, 10], rapid variability [11], and spatially resolved emission [12] indicate that particles gain energy efficiently within the jet flow. Among the proposed mechanisms, shock acceleration [13, 14] is widely considered the primary process. Internal shocks, formed by velocity variations in the outflow, or termination shocks at the interface with the ambient medium, can accelerate electrons and protons to TeV energies. Magnetic reconnection [15] and turbulent acceleration [16] may also contribute, particularly in regions with complex magnetic field structures, though their relative importance remains uncer-

tain. The accelerated particles undergo various energy loss processes that shape the observed emission. Synchrotron losses [17] dominate for high-energy electrons in strong magnetic fields, while inverse Compton scattering [9, 18] on ambient photon fields can produce gamma rays up to TeV energies. Hadronic interactions, particularly proton-proton collisions in dense environments, can lead to neutral pion decay [19], producing gamma rays at very high energies. Adiabatic expansion of the jet further contributes to particle cooling, affecting both the spectral and spatial distribution of the emission.

Microquasars are compact binary systems in our Galaxy, composed of a compact object—either a neutron star or a black hole—accreting matter from a stellar companion[20]. They are often associated with powerful, mildly relativistic jets that resemble[21], on smaller scales, the relativistic outflows observed in active galactic nuclei (AGN). Owing to their proximity and shorter variability timescales, microquasars serve as unique laboratories for studying jet physics, particle acceleration, and non-thermal emission processes under conditions analogous to those in AGN, but accessible on humanly observable timescales[7]. The microquasar SS 433 offers a particularly instructive case. Its jets, moving at approximately 0.26c [22], are mildly relativistic and precess with a period of 162 days [23–26], carrying a kinetic power of about 10^{39} erg/s [27]. The inner jets, within ~ 0.1 pc of the central binary [22, 28], have been extensively studied in the radio, optical, and X-ray bands, revealing their precession, collimation, and emission properties. In contrast, the outer jets, extending to ~ 25 pc, remain less understood. Observationally, they exhibit sudden re-brightening in X-rays and TeV gamma rays, suggesting localized particle acceleration or interactions with the surrounding medium. The contrast between the well-characterized inner jets and the enigmatic outer jets highlights the importance of resolving both spatial and spectral features to understand jet dynamics and radiation mechanisms.

SS 433 also stands out as an important object in

the very-high-energy regime. The High-Altitude Water Cherenkov (HAWC) observatory first reported TeV gamma-ray emission from the outer jets[29, 30], providing compelling evidence for efficient particle acceleration up to multi-TeV energies. More recently, the High Energy Stereoscopic System (H.E.S.S.) confirmed this detection with superior angular and energy resolution, enabling detailed morphological and spectral studies[13]. These observations revealed a striking energy-dependent morphology: while TeV photons are observed across extended regions of the jets, photons above ~ 10 TeV are confined to the vicinity of the jet bases. This result strongly disfavors a purely hadronic origin of the emission and instead points to efficient local particle acceleration, most likely at shock sites, coupled with rapid cooling.

In the ultra-high-energy ($E \ge 100 \text{ TeV}$) range, the Large High Altitude Air Shower Observatory (LHAASO)[31] has recently extended the observational window. In this region, LHAASO reported extended UHE gamma-ray emission from the central region of the system[32], coinciding with a giant gas cloud, suggesting a possible hadronic origin for at least part of the emission. Beyond SS 433, LHAASO has also detected UHE emission from several other black hole X-ray binaries, with spectra in some cases extending up to hundreds of TeV. These findings demonstrate that accreting black holes and their environments can act as extremely efficient cosmic accelerators, potentially contributing to Galactic cosmic rays in the PeV regime around the so-called "knee" of the spectrum. These observations establish SS 433 as a prototypical system for investigating jet-powered acceleration processes in compact binaries.

Yet, many key questions remain unresolved, including the physical origin of the jet re-brightening at large distances, the dominant radiative processes at work, and the dynamical properties of the outer jets. Addressing these open issues requires next-generation instruments that combine high sensitivity at multi-TeV energies with wide-field coverage and excellent angular resolution, particularly for photons above 100 TeV. The Large Array of imaging atmospheric Cherenkov Telescopes (LACT)[33], currently under construction at the same site as the LHAASO experiment, is designed to meet these requirements. LACT will naturally complement the wide energy coverage of the LHAASO air-shower array with its superior angular resolution. This synergy is particularly powerful: while LHAASO is capable of detecting photons well into the ultra-high-energy regime, its limited angular resolution prevents a detailed morphological study of extended sources such as the SS 433 jets. LACT, in contrast, will provide sub-degree imaging of the gamma-ray emission, enabling us to resolve the jet structure and directly probe the spatial dependence of the emission processes, thereby offering deeper insight into the physics of mildly relativistic microquasar jets.

By combining the broad energy coverage of LHAASO

with the high-resolution imaging of LACT, it becomes possible to confirm differences in emission above 100 TeV and in lower energy bands, identify localized acceleration regions, and study how particle transport shapes the extended emission. Building on the progress made by HAWC, H.E.S.S., and LHAASO, the motivation of this work is to present a preparatory study evaluating the scientific potential of LACT in advancing our understanding of SS 433—emphasizing how its instrumental strengths offer a unique opportunity to address long-standing questions about jet structure, emission origins, and particle acceleration in microquasar systems.

The paper is structured as follows. This Section reviews the current understanding of SS 433, with particular emphasis on its high-energy emission mechanisms and the open problems highlighted by recent observations. Section 2 introduces the LACT array, outlining its design features and performance advantages. Section 3 presents preliminary simulations and analysis strategies to evaluate the capability of LACT to detect and resolve the emission from SS 433. Finally, the last Section summarizes the key findings and discusses their implications for future observations of microquasars and Galactic particle acceleration.

OVERVIEW OF THE LACT ARRAY

LACT is designed as a next-generation facility capable of addressing the limitations of existing ground-based gamma-ray observatories. The array consists of 32 telescopes, each with a 6-meter diameter, and each telescope is equipped with a camera based on silicon photomultiplier (SiPM) technology, a well-validated solution previously demonstrated on LHAASO-WFCTA[34]. The use of SiPM cameras enables operation during moonlit nights, significantly increasing the effective observation time. LACT is optimized to combine high angular resolution with broad energy coverage, providing sub-degree imaging of extended sources such as SS 433's jets, while maintaining sensitivity down to energies below 1 TeV to allow observations of extragalactic sources and gamma-ray transients detected by LHAASO-WCDA[35].

For the full array, we adopt the LZA model with a zenith angle of 60° as the baseline observation configuration, optimized for PeVatrons and the highest-energy events. Increasing the effective area of Cherenkov telescopes at high energies by observing at large zenith angles (LZA) was proposed early on [36] and has been widely applied to existing IACTs. In addition to improving the effective area, LZA observations can also increase the sky coverage of IACTs. For example, at the LHAASO site, the Galactic Center (RA = $17^h45^m39.6^s$, Dec = 29° 00'22") can only be observed at zenith angles above 50° . At present, many instruments like VERITAS[37] and MAGIC[38] have verified LZA technology and applied it

for observation.

Compared to existing IACTs typically located at altitudes around 2000 m, the LHAASO site—at an elevation of 4400 m—benefits even more from large zenith angle observations. At this altitude, the shower maximum for 100 TeV gamma rays is very close to the ground, leading to a steep lateral distribution of Cherenkov photons and potential image leakage in the telescopes. In the LZA mode, however, the increased atmospheric depth between the shower maximum and the telescopes flattens the photon lateral distribution, resulting in smaller and higher-quality images[33].

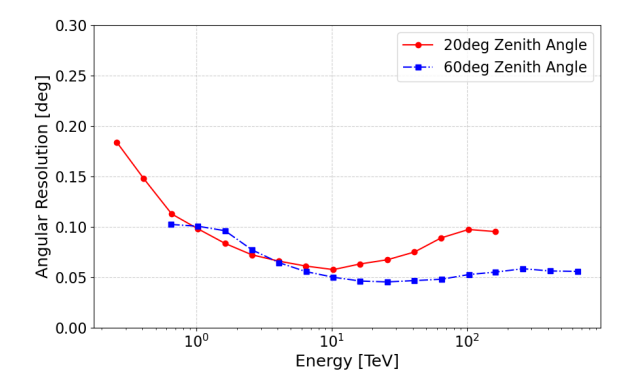
Traditional IACTs typically operate below 50° zenith angles to achieve the lowest possible energy threshold, for this purpose, we also adopt a dedicated small zenith angle model with a zenith angle of 20° for low-energy observations, aiming to ensure synergy with LHAASO-WCDA, particularly for time-domain γ -ray astronomy and extragalactic studies such as GRB and blazar observations. Compared with the LZA mode, small zenith angles enable lower threshold energies and improved performance for transient or extragalactic sources.

In previous work[33], detailed Monte Carlo simulations were carried out based on this design to determine the optimized LACT layout and evaluate the instrument performance in both large and small zenith angle modes. These studies provide estimates of the angular resolution and effective area, which are presented in Fig.1. In the following discussion, the instrument response functions (IRFs) used are derived from these two modes.

In the following part, we present simulations of LACT observations of SS 433, exploring its ability to detect and resolve the outer jets, reconstruct their spatial properties, and provide constraints on the underlying acceleration and emission mechanisms. These simulations serve as a preparatory step for future observations, demonstrating how LACT can bridge the gap between current gammaray observatories and advance our understanding of microquasar jets in the multi-TeV energy regime.

EVALUATION OF OBSERVATIONAL CAPABILITIES

To investigate the capabilities of LACT for observing the microquasar SS 433, we performed detailed simulations using the instrument response functions (IRFs) derived from the optimized array layout. The IRFs include all major performance characteristics, such as the effective area, angular resolution, energy dispersion, and background rejection efficiency (see Fig. 1). Simulations were conducted in both the 20°-zenith-angle mode, which maximizes sensitivity and angular resolution for sources near the zenith, and the 60°-zenith-angle mode, to account for observations at large zenith angles. By applying these IRFs to a realistic model of SS 433, including the



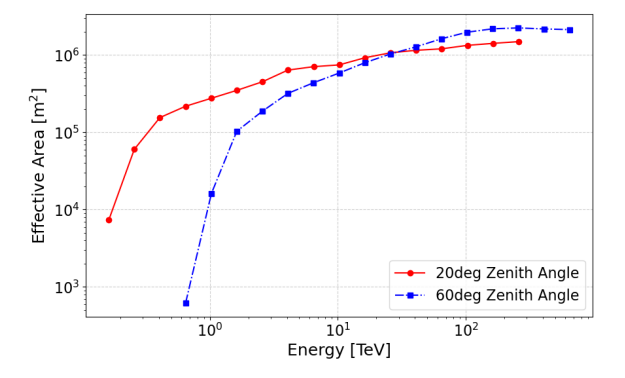


FIG. 1. Angular resolution and effective area of the LACT array as functions of energy for both large-zenith-angle (60°) and small- (20°) observation modes. The results are obtained from Monte-Carlo simulations based on the optimized array layout.

spatial distribution of the eastern and western jets, we are able to generate synthetic observations that closely resemble what could be obtained by the array under actual observing conditions.

Based on the source visibility calculated for the LHAASO site $(29^{\circ}21'27.6''N, 100^{\circ}08'19.6''E)$, we estimated the effective observation time available for SS 433 during the period of relatively good weather conditions, typically from October to the following April. This provides an approximate measure of the annual exposure window for the target, taking into account the site's latitude and the nighttime constraint defined by the Sun's altitude. In our calculation, nighttime was defined as the period when the Sun's altitude is below -18°(Astronomical Twilight), and the target's altitude was computed using the Astropy[39] coordinates framework. The cumulative observable hours under different zenith angle ranges $(0^{\circ}-50^{\circ})$ and $50^{\circ}-70^{\circ}$ are shown in Fig.2, illustrating how the accessible time gradually accumulates over the observing season. The results indicate that, over the six-month observing season, the effective observation time reaches more than 120 hours for small zenith angles (0°-50°) and over 200 hours for larger zenith angles (50°-70°), demonstrating that SS 433 can be well

observed from the LHAASO site.

A central aspect of the analysis is the study of the detection significance as a function of observation time. For each simulated dataset, significance maps were generated to evaluate the confidence level of source detection in both the eastern and western jets. To provide a realistic template for the simulations, the spatial and spectral properties of the jets were modeled based on H.E.S.S. observations, ensuring that the synthetic datasets reflect the best current knowledge of SS 433, which shown in Table.I. By tracking the accumulation of significance with increasing exposure, we can estimate the minimum observation time required for a robust detection of extended structures and localized high-energy features. This approach also allows the assessment of LACT's sensitivity to energy-dependent morphological characteristics, providing a means to distinguish between emission from compact acceleration regions near the jet bases and more extended radiation along the jet flow. Additionally, the nearby source HESS J1908+063 and the background model were included in the simulations to ensure a more realistic representation of the observational environment.

The simulations were carried out using Gammapy-1.3[40] analysis framework, extended to handle the IRFs specific to LACT. By combining the source model with the instrument response, we generated mock event lists and reconstructed both the spatial and spectral characteristics of the jets. which energy band is 10 - 300 TeV. Standard analysis procedures, including background estimation, event selection, and likelihood fitting, were applied to evaluate the detectability of the outer jets and the accuracy of the spectral reconstruction. The use of Gammapy enables a flexible and well-tested platform for this study, providing robust estimates of significance, flux, and morphology, while also allowing for direct comparison with existing H.E.S.S. results. To ensure that the results are statistically robust and not affected by random fluctuations, we performed 100 independent realizations for each observation time. For each simulation, the significance of the detection was calculated separately for the eastern and western jets of SS 433, allowing us to evaluate the expected detection confidence as a function of exposure. By aggregating the results from these repeated simulations, we were able to determine the mean significance and the corresponding 68% confidence intervals for each jet at different observation durations.

Preliminary simulations indicate that LACT can achieve high-confidence detection of the outer jets of SS 433 with relatively modest observation times. Specifically, a detection significance exceeding 3σ is expected after approximately 20 hours of exposure. For comparison, H.E.S.S. observations totaling around 200 hours have yielded significances of roughly 7.8σ and 6.8σ for the east and west jets, respectively. Representative results of these simulations, including the evolution of detec-

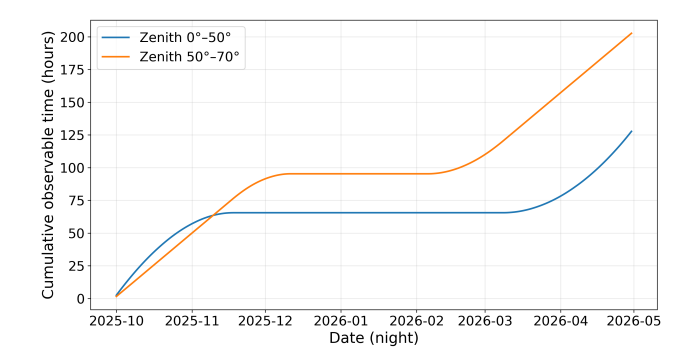


FIG. 2. Cumulative observable time of SS 433 from the LHAASO site between October and April. The curves show visibility under two zenith-angle ranges $(0^{\circ}-50^{\circ}$ and $50^{\circ}-70^{\circ})$. Nighttime is defined by the Sun's altitude below -18° .

TABLE I. Basic Information for jets of SS 433 from H.E.S.S observation spatial model above 10 TeV[13]. E_0 is the reference energy, ϕ_0 is the amplitude at the reference energy, and Γ is the photon spectral index. l and b are the Galactic longitude and latitude of the central position. Physical sizes for r are calculated assuming a distance of 5.5 kpc. The unit of ϕ_0 is 10^{-13} TeV⁻¹ cm⁻² s⁻¹.

Parameter	east	west	
$l (\deg)$	$39.840^{\pm0.031}$	$39.560^{\pm0.010}$	
b (deg)	$-2.643^{\pm0.038}$	$-1.951^{\pm0.011}$	
$r ext{ (deg)}$	$0.013^{\pm0.029}$	=	
ϕ_0		$2.83^{\pm 0.70_{\text{stat.}} \pm 0.39_{\text{syst.}}}$	
Γ	$2.19^{\pm 0.12_{\text{stat.}} \pm 0.12_{\text{syst.}}}$	$2.40^{\pm 0.15_{\text{stat.}} \pm 0.13_{\text{syst.}}}$	

tion significance for the east and west jets, are presented in Figure.4. These results demonstrate that LACT can achieve high-confidence detection for both the eastern and western jets within reasonable observation times, while also providing good spatial resolution for a clear observation of both jets.

Another important observations of SS 433 is that LHAASO's results above 100 TeV point towards an extended source LHAASO J1911+0513[32], the basic information is listed in Table.II), and the spectrum of the extended source above 100 TeV is

$$\frac{dN}{dE} = (3.45 \pm 1.61) \times 10^{-16} \left(\frac{E}{50 \text{ TeV}}\right)^{-3.96 \pm 0.25}$$
 (TeV⁻¹ cm⁻² s⁻¹)

To investigate the capability of LACT to distinguish different emission scenarios of SS 433, we adopted a consistent analysis framework based on the three-source model inferred from the LHAASO observation [32]. Using this model as the input source template, we simulated LACT observations at a zenith angle of 60° with the corresponding IRFs, and fitted the simulated data

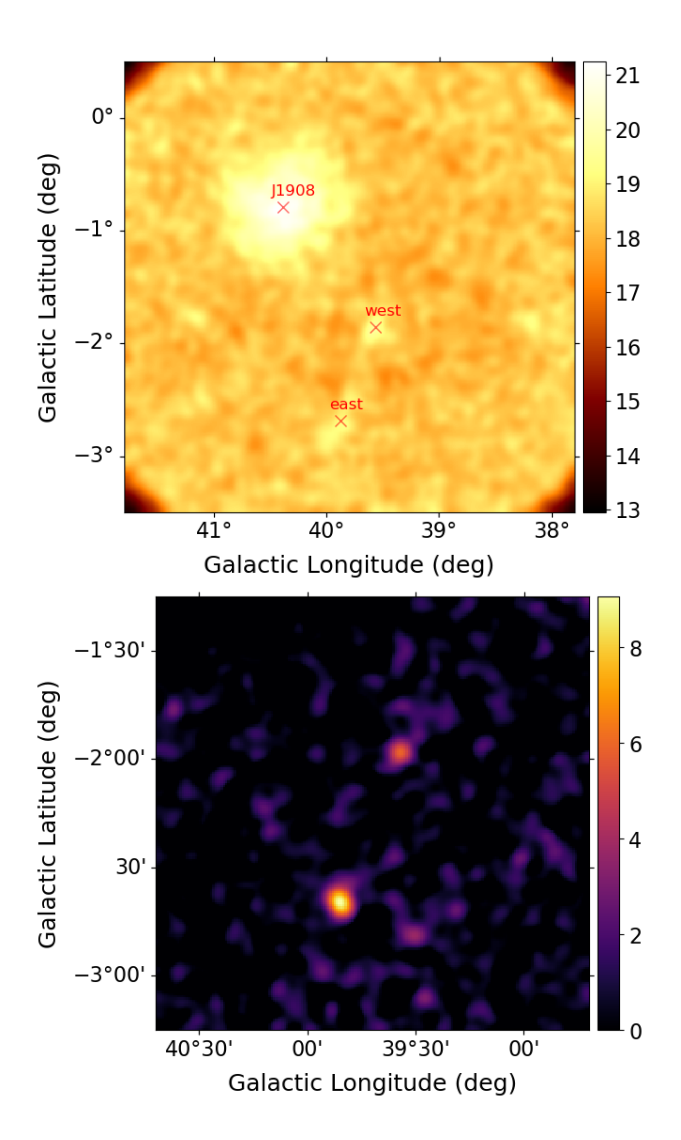


FIG. 3. Top: A counts map of the SS 433 eastern and western jets from an 100-hour simulated observation. Bottom: The corresponding significance map in SS 433 region, where the significance is represented as the square root of the TS value.

TABLE II. Basic properties of the source LHAASO J1911+0513, which observed by LHAASO in SS 433 region at energies above 100 TeV[32]. The table lists the original equatorial coordinates (RA, Dec) and the radius parameter r_{39} , as well as the corresponding galactic coordinates (l, b) of the source center. At 100 TeV, 1 CU = 6.1×10^{-17} TeV⁻¹cm⁻²s⁻¹[41].

coordinate	position(deg)	$r_{39}(\deg)$	flux
$\frac{\overline{(RA,Dec)}}{(l,b)}$	$(287.89^{\pm0.11}, 5.22^{\pm0.12})$ (39.87, -2.08)	$0.32^{\pm0.09}$	0.32 CU (100 TeV)

with both the LHAASO and H.E.S.S. spectral models to assess their distinguishability.

We first focused on photons with energies above 100 TeV to test LACT's performance in the ultra-high-energy regime. The difference in detection significance

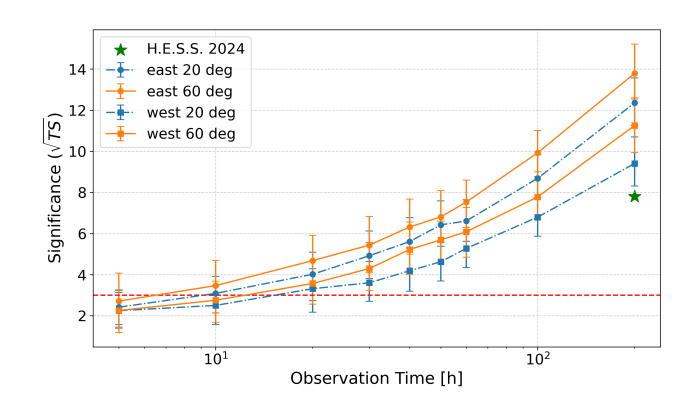


FIG. 4. The detection significance of the SS 433 eastern and western jets as a function of observation time. The red dashed line indicates the 3σ threshold. Each data point represents the mean of total simulations, with error bars corresponding to the 68% confidence interval. The star reprents the result of H.E.S.S.(east jet, 7.8σ)[13].

between the two models is shown in Fig. 6. As expected, the detection significance gradually increases with exposure time; however, due to the steep power-law spectrum, the flux above 100 TeV is too low for the results to become statistically significant within a reasonable observation time.

Considering the LHAASO results (Fig. 1e in [32]), which suggest that the hadronic-origin emission still makes a substantial contribution below 100 TeV, we extended the spectral range of the LHAASO-like extended source by including this additional hadronic component. In the simulation, we constructed a three-component model consisting of the central hadronic component and the two leptonic jet components, following the spatial and spectral characteristics inferred from LHAASO observations. The same three-component configuration was adopted in the fitting procedure to evaluate how well LACT can recover the central hadronic emission under different energy thresholds and observation times.

As shown in Fig. 7, for energies above 30 TeV, LACT would be able to marginally detect (3σ significance) the central hadronic component after about 50 h of observation. When the threshold is increased to 50 TeV, achieving a similar significance would require approximately 100 h of exposure. At higher energies (e.g., above 100 TeV), although the hadronic component becomes increasingly dominant relative to the leptonic emission, the photon statistics are too limited for a significant detection. These results indicate that LACT's excellent angular resolution enables it to start resolving the hadronic-origin emission in the tens-of-TeV range within a feasible observation time.

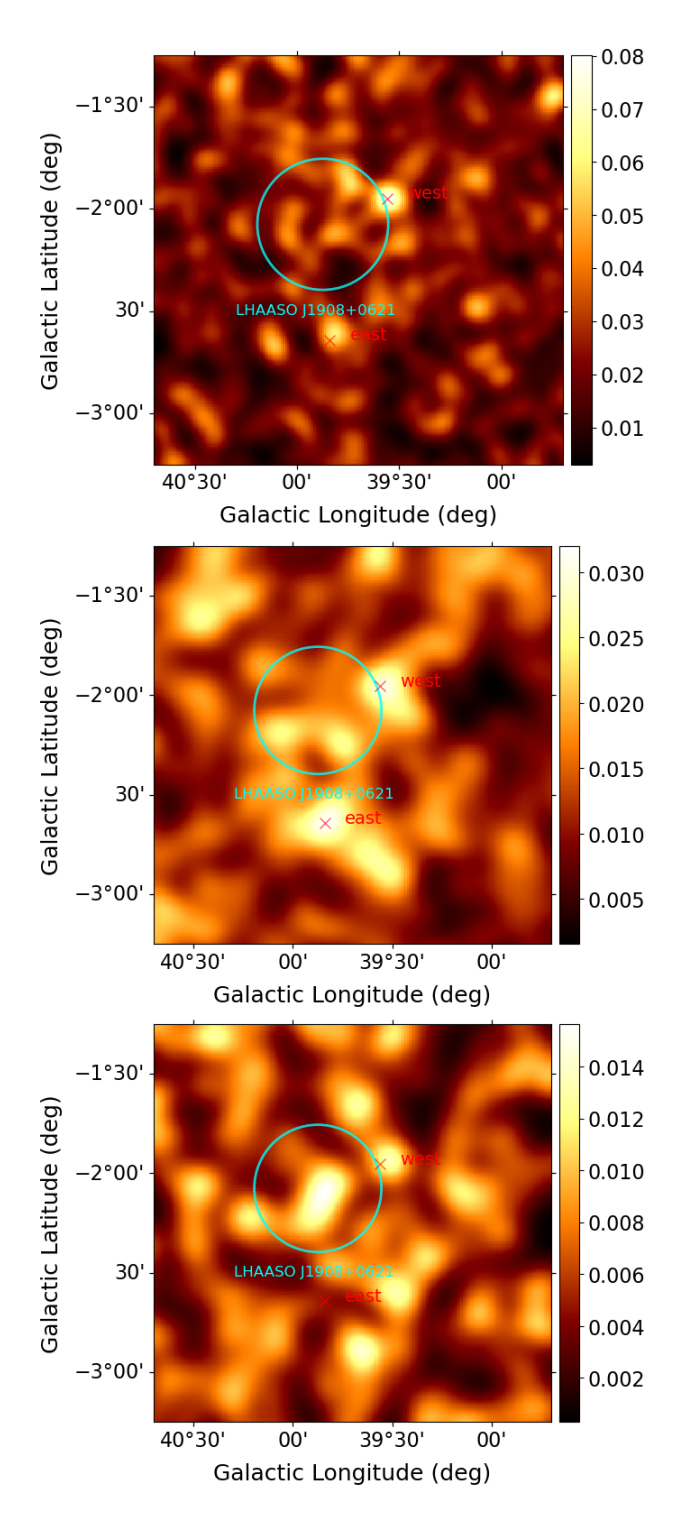


FIG. 5. Simulated LACT counts maps for SS 433 based on the three-source model inferred from LHAASO observations. From top to bottom: photon energies above 30 TeV, 50 TeV, and 100 TeV. The red crosses mark the positions of the two jet regions, while the cyan circle indicates the location and approximate extent of the extended source reported by LHAASO. All maps correspond to one 100-hour observation in the 60°-zenith-angle mode using the same IRFs. At energies above 100 TeV, the very low photon counts lead to noticeable irregular fluctuations dominated by the background.

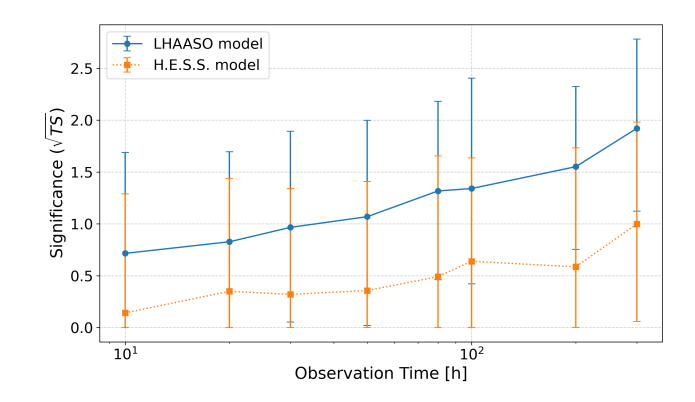


FIG. 6. Difference in significance between fits with H.E.S.S. and LHAASO templates for events above 100 TeV, with the mean significance as a function of observation time, assuming the source spectrum extends to energies below 100 TeV. Each data point represents the mean of total simulations, performed in the 60° zenith-angle mode.

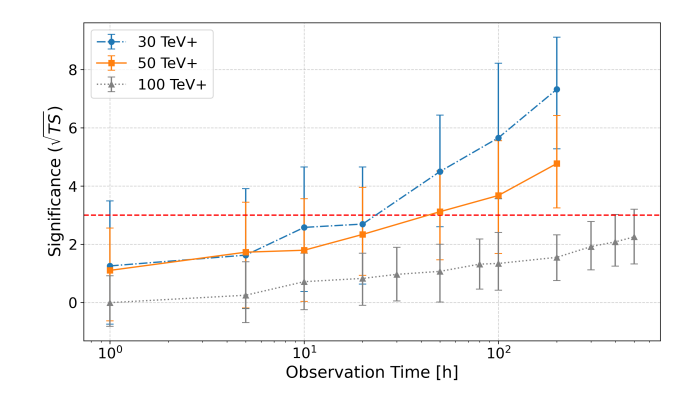


FIG. 7. Detection significance of the central hadronic component as a function of observation time for different energy thresholds. The curves correspond to simulated LACT observations above 30 TeV, 50 TeV, and 100 TeV, respectively.

CONCLUTION

In this work, we have explored the scientific potential of the LACT for investigating the microquasar SS 433, with particular emphasis on its extended outer jets and their high-energy non-thermal emission. SS 433 represents one of the most remarkable laboratories for studying relativistic jet physics within our Galaxy, providing a unique opportunity to probe particle acceleration and radiation processes under extreme conditions. Although instruments such as H.E.S.S., HAWC, and LHAASO have provided crucial evidence for very-high- and ultra-high-energy γ -ray emission from this system, their limitations in angular resolution, sensitivity, or energy coverage still prevent a detailed morphological and spectral dissection of the jet regions.

Based on the source visibility calculations, we estimate

that at the LHAASO site, during the favorable observing season from October to April, the available observation time amounts to about 120 hours for small zenith angles (0°-50°) and more than 200 hours for large zenith angles (50°-70°), as shown in Fig.2. Our simulation results show that LACT can effectively resolve the eastern and western jet structures of SS 433, achieving a detection significance of approximately 5σ within 30 hours in the 10–300 TeV range, with significantly higher sensitivity than current H.E.S.S. observations, as shown in Fig.4. At energies above 100 TeV, LACT is capable of detecting the extended emission reported by LHAASO, but due to the steep spectral decline, substantially longer exposures are required to reach comparable significance (see Fig.6). If SS 433 indeed contains a hadronic-origin component, as suggested by the extended emission observed by LHAASO, LACT would be capable of detecting the corresponding gamma-ray emission from the central region above 30 TeV, reaching a marginal significance of about 3σ after 50 h of observation and about 100 h above 50 TeV as shown in Fig.7. This demonstrates that LACT can start to resolve the hadronic-origin emission within a realistic observation time, even though higher-energy detections are limited by photon statistics.

Overall, our results demonstrate that LACT will be a powerful instrument for high-resolution studies of microquasar jets and other extended γ -ray sources. The simulations presented in this work establish a quantitative basis for future observational campaigns, providing guidance for the optimization of exposure strategies and observation modes in different zenith-angle configurations. By resolving energy-dependent morphological features and distinguishing localized acceleration zones, LACT can offer new insights into particle transport, cooling, and emission processes that are currently beyond the reach of existing instruments. Beyond SS 433, the simulation framework and analysis approach developed here can be readily applied to a wide range of Galactic and extragalactic γ -ray sources, opening new opportunities for investigating particle acceleration and non-thermal phenomena in extreme astrophysical environments.

ACKNOWLEDGMENT

Rui-zhi Yang is supported by the natural science Fundation of Sichuan Province under grant 2025ZNS-FSC0065, and by the NSFC under grant 12393854, 12588101 and 12041305. Rui-zhi Yang gratefully acknowledges the support of the Cyrus Chun Ying Tang Foundations and the Tianfu Talent project. We would also like to thank Yanhong Yu and Wenyu Cao for their valuable assistance and insightful discussions regarding the LHAASO data analysis and science related to SS 433.

- yangrz@ustc.edu.cn
- H. D. Curtis, Descriptions of 762 nebulae and clusters photographed with the crossley reflector, Publications of Lick Observatory, vol. 13, pp. 9-42 13, 9 (1918).
- [2] K. G. Jansky, Radio waves from outside the solar system, Nature **132**, 66 (1933).
- [3] R. Jennison and M. Das Gupta, Fine structure of the extra-terrestrial radio source cygnus i, Nature 172, 996 (1953).
- [4] M. Schmidt, 3c273: a star-like object with large redshift.", A Century of Nature, Twenty One Discoveries That Changed Science and the World (1963).
- [5] C. Hazard, M. Mackey, and A. Shimmins, Investigation of the radio source 3 c 273 by the method of lunar occultations, Nature 197, 1037 (1963).
- [6] H. Falcke and P. L. Biermann, Galactic jet sources and the agn connection., Astronomy and Astrophysics, v. 308, p. 321-329 308, 321 (1996).
- [7] T. Belloni, The jet paradigm: from microquasars to quasars, Vol. 794 (Springer, 2009).
- [8] J. Davelaar, H. Olivares, O. Porth, T. Bronzwaer, M. Janssen, F. Roelofs, Y. Mizuno, C. M. Fromm, H. Falcke, and L. Rezzolla, Modeling non-thermal emission from the jet-launching region of m 87 with adaptive mesh refinement, Astronomy & Astrophysics 632, A2 (2019).
- [9] F. C. Jones, Calculated spectrum of inverse-comptonscattered photons, Physical Review **167**, 1159 (1968).
- [10] F. De Colle, W. Lu, P. Kumar, E. Ramirez-Ruiz, and G. Smoot, Thermal and non-thermal emission from the cocoon of a gamma-ray burst jet, Monthly Notices of the Royal Astronomical Society 478, 4553 (2018).
- [11] M. V. Barkov, F. A. Aharonian, S. V. Bogovalov, S. R. Kelner, and D. Khangulyan, Rapid tev variability in blazars as a result of jet—star interaction, The Astrophysical Journal 749, 119 (2012).
- [12] V. Schulz-Von Der Gathen, L. Schaper, N. Knake, S. Reuter, K. Niemi, T. Gans, and J. Winter, Spatially resolved diagnostics on a microscale atmospheric pressure plasma jet, Journal of Physics D: Applied Physics 41, 194004 (2008).
- [13] H. Collaboration*†, F. Aharonian, F. A. Benkhali, J. Aschersleben, H. Ashkar, M. Backes, V. B. Martins, R. Batzofin, Y. Becherini, D. Berge, et al., Acceleration and transport of relativistic electrons in the jets of the microquasar ss 433, Science 383, 402 (2024).
- [14] F. C. Jones and D. C. Ellison, The plasma physics of shock acceleration, Space Science Reviews 58, 259 (1991).
- [15] H. Sakemi, M. Machida, T. Akahori, H. Nakanishi, H. Akamatsu, K. Kurahara, and J. Farnes, Magnetic field analysis of the bow and terminal shock of the ss 433 jet, Publications of the Astronomical Society of Japan 70, 27 (2018).
- [16] A. Panferov, Simulation of kinematics of ss 433 radio jets that interact with the ambient medium, Astronomy & Astrophysics 562, A130 (2014).
- [17] C. D. Dermer and A. M. Atoyan, X-ray synchrotron spectral hardenings from compton and synchrotron losses in extended chandra jets, The Astrophysical Journal 568, L81 (2002).

- [18] F. C. Jones, Inverse compton scattering of cosmic-ray electrons, Physical Review 137, B1306 (1965).
- [19] S. Stephens and G. Badhwar, Production spectrum of gamma rays in interstellar space through neutral pion decay, Astrophysics and Space Science 76, 213 (1981).
- [20] I. F. Mirabel, Microquasars, Comptes Rendus Physique 8, 7 (2007).
- [21] V. Bosch-Ramon and D. Khangulyan, Understanding the very-high-energy emission from microquasars, International Journal of Modern Physics D 18, 347 (2009).
- [22] K. M. Blundell and M. G. Bowler, Symmetry in the changing jets of ss 433 and its true distance from us, The Astrophysical Journal 616, L159 (2004).
- [23] A. Fabian and M. Rees, Ss 433: a double jet in action?, Monthly Notices of the Royal Astronomical Society 187, 13P (1979).
- [24] M. Milgrom, On the interpretation of the large variations in the line positions in ss433, Astronomy and Astrophysics, vol. 76, no. 1, June 1979, p. L3-L6. 76, L3 (1979).
- [25] B. Margon, H. Ford, J. Katz, K. Kwitter, R. Ulrich, R. Stone, and A. Klemola, The bizarre spectrum of ss 433, Astrophysical Journal, Part 2-Letters to the Editor, vol. 230, May 15, 1979, p. L41-L45. 230, L41 (1979).
- [26] R. Hjellming and J. KJ, An analysis of the proper motions of ss 433 radio jets, Reprints-National Radio Astronomy Observatory, Green Bank, W. Va. Series A. 246, 1281 (1981).
- [27] B. Margon, Relativistic jets in ss 433, Science 215, 247 (1982).
- [28] R. Spencer, A radio jet in ss433, Nature **282**, 483 (1979).
- [29] L. Olivera Nieto, Resolving particle acceleration and transport in the jets of the microquasar SS 433 with HESS and HAWC, Ph.D. thesis (2023).
- [30] R. Alfaro, C. Alvarez, J. Arteaga-Velázquez, D. A. Rojas, H. A. Solares, R. Babu, E. Belmont-Moreno, A. Bernal, K. Caballero-Mora, T. Capistrán, et al., Spectral study of very-high-energy gamma rays from ss 433 with hawc, The Astrophysical Journal 976, 30 (2024).
- [31] C. Zhen, C. Ming-Jun, C. Song-Zhan, H. Hong-Bo, L. Cheng, L. Ye, M. Ling-Ling, M. Xin-Hua, S. Xiang-Dong, W. Han-Rong, et al., Introduction to large high altitude air shower observatory (lhaaso), Chinese Astron-

- omy and Astrophysics 43, 457 (2019).
- [32] L. Collaboration et al., Ultrahigh-energy gamma-ray emission associated with black hole-jet systems, arXiv preprint arXiv:2410.08988 (2024).
- [33] Z. Zhang, R. Yang, S. Zhang, Z. Xie, J. Liu, L. Yin, Y. Wang, L. Ma, and Z. Cao, Layout optimization and performance of large array of imaging atmospheric cherenkov telescope (lact), arXiv preprint arXiv:2409.14382 (2024).
- [34] F. Aharonian, Q. An, Axikegu, L. Bai, Y. Bai, Y. Bao, D. Bastieri, X. Bi, Y. Bi, H. Cai, et al., Construction and on-site performance of the lhaaso wfcta camera, The European Physical Journal C 81, 657 (2021).
- [35] S. Hu, G. Xiang, M. Zha, Z. Yao, et al., The first lhaaso catalog of gamma-ray sources below 25tev, (2023).
- [36] A. Konopelko, F. Aharonian, M. Hemberger, W. Hofmann, J. Kettler, G. Pühlhofer, and H. J. Völk, Effectiveness of tev-ray observations at large zenith angles with a stereoscopic system of imaging atmospheric cerenkov telescopes, Journal of Physics G: Nuclear and Particle Physics 25, 1989 (1999).
- [37] C. Adams, W. Benbow, A. Brill, R. Brose, M. Buchovecky, M. Capasso, J. Christiansen, A. Chromey, M. Daniel, M. Errando, et al., Veritas observations of the galactic center region at multi-tev gamma-ray energies, The Astrophysical Journal 913, 115 (2021).
- [38] V. A. Acciari, S. Ansoldi, L. Antonelli, A. A. Engels, D. Baack, A. Babić, B. Banerjee, U. B. De Almeida, J. Barrio, J. B. González, et al., Magic very large zenith angle observations of the crab nebula up to 100 tev, Astronomy & astrophysics 635, A158 (2020).
- [39] T. A. Collaboration, The astropy project: Sustaining and growing a community-oriented open-source project and the latest major release (v5.0) of the core package*, The Astrophysical Journal 935, 167 (2022).
- [40] A. Donath, R. Terrier, Q. Remy, A. Sinha, C. Nigro, F. Pintore, B. Khélifi, L. Olivera-Nieto, J. E. Ruiz, K. Brügge, et al., Gammapy: A python package for gamma-ray astronomy, Astronomy & Astrophysics 678, A157 (2023).
- [41] Z. Cao, F. Aharonian, Q. An, Axikegu, L. Bai, Y. Bai, Y. Bao, D. Bastieri, X. Bi, Y. Bi, et al., Ultrahigh-energy photons up to 1.4 petaelectronvolts from 12 γ-ray galactic sources, Nature 594, 33 (2021).